Proton-Induced Damage on 2-Aminooxazole, a Potential Prebiotic Compound

ARTICLE *in* THE JOURNAL OF PHYSICAL CHEMISTRY A · JANUARY 2015

Impact Factor: 2.69 · DOI: 10.1021/jp511658n · Source: PubMed

1 AUTHOR:

Marie-Christine Bacchus-Montabonel
Claude Bernard University Lyon 1
115 PUBLICATIONS **904** CITATIONS

SEE PROFILE

THE JOURNAL OF PHYSICAL CHEMISTRY A

Article

pubs.acs.org/JPCA

Proton-Induced Damage on 2-Aminooxazole, a Potential Prebiotic Compound

Marie-Christine Bacchus-Montabonel*

Institut Lumière matière, UMR5306 Université Lyon 1-CNRS, Université de Lyon, 69622 Villeurbanne Cedex, France

Supporting Information

ABSTRACT: Among the complex organic molecules detected in space, in the interstellar medium, on meteorites or comets, special interest is devoted to the potentially exobiologic-relevant species. In the hypothesis, widely discussed, of a possible exogen origin of life, the transport of such compounds and their survival is indeed a fundamental question. Recently, suggestion has been made that 2-aminooxazole could be a possible precursor of RNA nucleotides on early earth and its stability to UV radiation or to collisions may be determinant. We have thus undertaken a detailed theoretical study of the charge transfer collision dynamics induced by the impact of 2-aminooxazole with protons, which could be an important process in particular in proton-rich environments. The theoretical treatment has been developed through *ab initio* quantum chemistry molecular calculations followed by semiclassical collision dynamics. The results are compared to previous investigations on DNA and RNA building blocks in order to extract some qualitative trends in the damage of prebiotic species under spatial radiation.

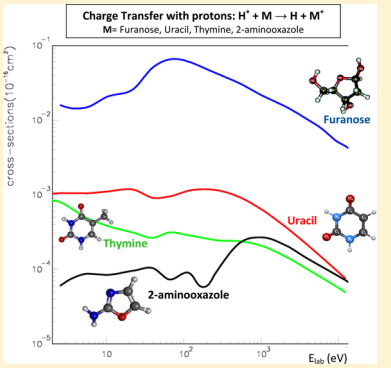

1. INTRODUCTION

Since the early Miller and Hurey experiments aiming to produce amino acids from mixtures of simple molecules,[1,2] prebiotic chemistry has worked to understand how those compounds necessary for the origin of life could be formed in the interstellar medium or on ice grains. Presently, observations have succeeded to detect a number of those complex organic molecules in the interstellar medium, as well as in comets or meteorites, and special interest is devoted to those molecules that could be prebiotic precursors in the formation of building blocks of life.[3,4] In the "RNA world" hypothesis generally accepted,[5,6] RNA must have been formed from purely chemical processes, but direct experimental support from ribose and nucleobases reaction failed.[7] However, an efficient and selective sequence has been proposed recently in the group of J. Sutherland leading to pyrimidine ribonucleotides under prebiotic conditions by reaction of cyanamide and glycolhaldehyde.[8−10] The key step of this process is the formation of 2-aminooxazole, which could be a fundamental prebiotic species. Great interest has thus been devoted to this intermediate with, first of all, the analysis of the possibility of observation of the compound by microwave spectroscopy.[11] The detailed mechanism of the formation of 2-aminooxazole in prebiotic conditions has also been analyzed by density functional calculations showing the importance of phosphate catalysis,[12] and the possible radiationless decay pathways have been investigated as UV irradiation is a crucial factor in the proposed reaction sequence.[13]

The prolonged UV irradiation indeed appears as a key factor in the reaction scheme of 2-aminooxazole formation in prebiotic conditions.[8,9,13] This points out a quite fundamental question concerning the origin of life, which is how to understand the selectivity of a small number of given molecules at the beginning of life. Intense UV irradiation could be a plausible important environment factor. Effectively, since amino acids have been discovered in the Murchison meteorite,[14] the assumption of an exogen origin for life has been suggested, which raised intense discussions. In such hypothesis, the survival and transport of prebiotic building blocks, their thermic desorption from the mantle of ice grains, and above all their resistance to spatial radiation as solar UV radiations or cosmic rays are fundamental open questions.[15,16]

Within a more general context, radiation damage to biological species has been shown to be driven not only by photon radiation, but also by secondary particles as low-energy electrons, OH radicals, or even ions that are generated along the ionizing radiation track.[17,18] In that way, we have considered collisions of biological building blocks with given ions; mainly protons or carbon ions with regard to their abundance or their implication in cancer treatments. Such studies may be supported by time-of-flight experiments in the gas-phase, generally performed at keV energies[19−21] but also at lower energies in the eV range.[22,23] Those experimental investigations may be completed by theoretical approaches; we have considered in particular collisions of carbon ions with DNA building blocks for eV to keV energies.[24−29] If one considers astrophysical environments, such ion-biomolecule collisions may occur for a very wide range of temperatures,[30] from (∼meV) in the interstellar medium, to 10^4 K (∼10 eV) or more in evolved stars, and can reach up to MeV energies for

Received: November 21, 2014
Revised: January 9, 2015

DOI: 10.1021/jp511658n
J. Phys. Chem. A XXXX, XXX, XXX−XXX

nucleus of high energy in cosmic rays. With regard to the abundance of hydrogen in space, consideration of collisions of prebiotic species with protons appears determinant. This would be a fundamental process in H II regions of space. We have investigated in a previous paper the collision of protons with the DNA and RNA building blocks, pyrimidine nucleobases, and deoxyderibose sugar moiety in order to compare their behavior and try to extract some qualitative trends on their resistance in proton-rich environments.[31] A strong sensitivity to radiations has been pointed out, in particular for the pyrimidine nucleobases. Furthermore, the process appears significantly dependent on the conformation of the biomolecule as the 2-deoxy-D-ribose exhibits a relatively higher resistance to radiations in its five-membered furanose form than in the six-membered pyranose one.[31,32] The 2-aminooxazole consisting of a NH_2 group bounded to the five-membered oxazole ring, the same resistance could be expected for such compound, which would support the survival of such a prebiotic species, and thus its possible important role in the early life. A similar analysis has thus been developed to look at the behavior of the 2-aminooxazole in collisions with protons in order to establish a comparative study.

Considering collisions of ions with biomolecular targets, different processes must be taken into account. First of all excitation and ionization of the molecular target, either by direct ionization or by charge transfer from the projectile ion toward the biomolecule, then fragmentation of the ionized species. Experimental studies provide mainly fragmentation patterns, which may inform on the fragmentation mechanism of the biomolecular target after ionization.[19−23] From a theoretical point of view, dynamical treatments on ionized species may be developed accordingly, taking into account that ionization can be considered as almost instantaneous with regard to the fragmentation time.[33,34] However, such an ionization step is quite important and cannot be neglected. In particular, ionization by charge transfer is a determinant process that may be studied theoretically in the framework of the molecular representation of the collisions. We have thus proposed a quantum molecular treatment that has shown its efficiency for such ion-biomolecule systems. The potentials and nonadiabatic coupling matrix elements between the different molecular states involved in the charge transfer process are determined by means of ab initio methods, and the collision is performed using semiclassical approaches valid in a wide collision energy domain.[35−37] Such treatment has been extended for collisions of protons on 2-aminooxazole. The calculation has been performed at the level of theory already used in previous studies on DNA and RNA building blocks in order to extract general features for radiation damage.

2. THEORETICAL TREATMENT

a. Molecular Calculations. In the molecular description of the collision, the charge transfer process is described by the evolution of the ion-target quasi-molecular system. For complex compounds such as those involving biomolecules, a model may be defined using the one-dimensional reaction coordinate approximation.[38−40] The ion-biomolecular target collision system may therefore be considered as a quasi-diatomic molecule moving along the reaction coordinate associated with the distance R between the projectile ion and the center-of-mass of the target. As already pointed out, charge transfer is a very fast process, and electronic transitions can thus be assumed to be much faster than vibrational and rotational movements of the biomolecule. The process may thus be handled in the framework of the sudden-approximation hypothesis by keeping the target geometry frozen during the collision time. Although very crude, such an approach neglecting the internal motions of the biomolecular target has been shown to provide quite reliable results for very fast processes such as the charge transfer ionization we are considering here.[25]

The collision system is displayed in Figure 1a. The five-membered ring is in the vertical xy plane. The molecular levels involved in the process are calculated with regard to the reaction coordinate R along z in the perpendicular geometry, and in the xy ring plane along x and y. A detailed description of the orientation of the coordinate axes is given in Figure 1b. The molecular calculations are carried out by means of the MOLPRO code.[41] The geometry of the 2-aminooxazole ground state has been optimized at the MP2 and CASSCF (Complete Active Space Self Consistent Field) levels of theory generally used in optimization calculations. In order to compare these results to calculations on nucleobases and 2-deoxy-D-ribose compounds, the 6-311G** basis of atomic orbitals considered in previous works was chosen. Both structures are in good agreement with parameters deduced from microwave spectra and previous optimized geometries.[11,13] The present optimized geometries are provided as Supporting Information (Tables S1 and S2). The ionized species have also been optimized (Supporting Information, Table S3), and corresponding adiabatic and vertical ionization potentials are displayed in Table 1 together with pyrimidine nucleobase data. The ionization potentials for 2-aminooxazole appear lower

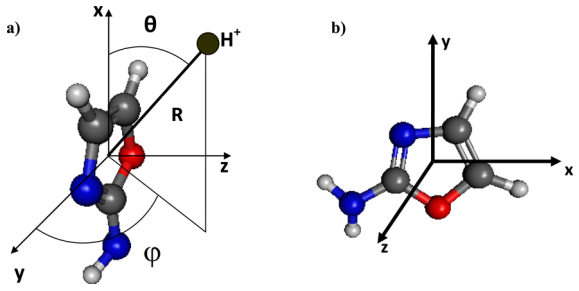

Figure 1. (a) Internal coordinates for the H^+ + 2-aminooxazole system. The five-membered ring is in the xy plane, and the z axis is perpendicular to the ring plane with origin at the center-of-mass of the ring. The angle φ corresponds to the angle between the y axis and the projection of H^+ on the yz plane. (b) Detail of the geometry of the 2-aminooxazole and orientation of the coordinate frame. The z axis is perpendicular to the xy ring plane.

Table 1. Ionization Potentials of 2-Aminooxazole at the CASSCF/6-311G Level of Theory[a]**

	vertical		adiabatic	
		experiment		experiment
uracil	9.56[b] 9.47[d]	9.50[b,d]	9.34[b] 9.21[d]	9.35[b,d]
thymine	9.09[c] 9.02[d]	9.14[d]	8.73[c] 8.74[d]	8.95[d]
2-aminooxazole	8.38		7.69	

[a]Comparison with pyrimidine nucleobases (in eV). [b]Reference 24. B3LYP/6-31G** calculations and experimental data. [c]Reference 27. CASSCF/6-311G** calculations. [d]Reference 42. B3LYP/6-311+G-(2df,p) calculations and experimental data.

DOI: 10.1021/jp511658n
J. Phys. Chem. A XXXX, XXX, XXX−XXX

than those of uracil and thymine, around 8 eV compared to values around 9 eV for nucleobases. To our knowledge, no experimental data are available in the literature for 2-aminooxazole. The MP2 optimized geometry has been used in the collision treatment. Molecular calculations of the 2-aminooxazole + H^+ system have been performed in the C1 symmetry group with no symmetries taking account of all electrons and using Cartesian coordinates with origin at the center-of-mass of the oxazole five-membered ring. The potential energies and nonadiabatic coupling matrix elements (NACME) have been calculated by state-average CASSCF/CASPT2 methods for a large number of R values between 0.5 and 9 Å. The potential energies have been extrapolated to reach the asymptotic limit. The active spaces involve the six valence orbitals of highest energy, mainly constructed on the $2p_x$, $2p_y$, $2p_z$ orbitals on nitrogen N1, the $2p_z$ orbitals on carbon atoms C1 and C2 giving rise to the π_{C1C2} orbital (see Figure 1b), with, of course, the 1s orbital on the colliding hydrogen atom. The 1s orbitals on oxygen, nitrogen and carbon have been considered as frozen cores. The 6-311G** basis set has been used in all calculations.

Charge transfer between the entrance and exit channels is linked to the nonadiabatic interactions in the neighborhood of the avoided crossings. An accurate calculation of the position and height of NACME's is thus determinant.[43,44] The nonadiabatic radial coupling matrix elements between states of the same symmetry have been calculated numerically using the finite difference technique:

$$g_{KL}(R) = \langle \psi_K | \partial/\partial R | \psi_L \rangle = \left\langle \psi_K(R) \middle| \lim_{\Delta \to 0} \frac{1}{\Delta} \middle| \psi_L(R+\Delta) - \psi_L(R) \right\rangle \quad (2\text{-}1)$$

As eigenfunctions $|\psi_K(R)\rangle$ and $|\psi_L(R)\rangle$ are orthogonal for $K \neq L$, the present expression reduces to

$$g_{KL}(R) = \langle \psi_K | \partial/\partial R | \psi_L \rangle = \lim_{\Delta \to 0} \frac{1}{\Delta} \langle \psi_K(R) | \psi_L(R+\Delta) \rangle \quad (2\text{-}2)$$

Extended tests for the choice of the step Δ have been previously performed showing that a value $\Delta = 0.0012$ au may provide an accurate stability for the differentiation procedure.[45] For numerical accuracy, a three-point numerical finite difference is preferred, taking the center-of-mass of the biomolecular target as the origin of the electronic coordinates.

b. Collision Dynamics. Semiclassical methods have been used in the collision treatment. As pointed out in theprevious paragraph, calculations have been performed in the sudden approximation hypothesis assuming much faster electronic transitions than vibration and rotation motions. The geometry of the biomolecular target thus remains frozen in its ground state during the collision time, and the total and partial cross sections, relying on electronic transitions, are calculated as in an ion−atom collision by resolution of the impact-parameter equation. Such a simple approach may provide quite valid results for energies above ∼10 eV/amu[46] for which typical vibrational and moreover rotational times are assumed to be much longer than the collision time,[47] as we showed previously for carbon ion/uracil collisions.[25] With regard to our recent studies comparing time-dependent wave packet dynamics and semiclassical approaches in ion-atom processes,[48,49] extension of the collisional treatment to lower collision energies could be reliable down to the eV domain.[28] The semiclassical method is thus expected to provide at least the order of magnitude of charge transfer cross sections in a wide impact energy range.

In the semiclassical method, a classical trajectory is considered for the nuclei $R(t) = b + vt$, where b is the impact parameter and v is the velocity. The time-dependent Schrödinger equation thus reduces to

$$\left(H^{el}[r, R(t)] - i\frac{\partial}{\partial t} \right) \times \Psi(r, b, v, t) = 0 \quad (2\text{-}1)$$

where H^{el} is the electronic Born−Oppenheimer Hamiltonian and r is the electronic coordinates. The resolution for each velocity v and impact parameter b is performed by expanding the total wave function on the adiabatic eigenfunctions $\psi_{K\Lambda}$ of H^{el} with eigenvalues $\varepsilon_{K\Lambda}$, where K is the number of electronic states $\psi_{K\Lambda}$ and Λ is the quantum number corresponding to the projection of the total electronic orbital angular momentum $\mathbf{L}$ on the molecular axis:

$$\Psi(r, b, v, t) = \sum_{K\Lambda} a_{K\Lambda}(b, v, t) \psi_{K\Lambda}[r, R(t)] \times \exp\left(-i \int_0^t \varepsilon_{K\Lambda}[R(t')]\, dt'\right) \quad (2\text{-}2)$$

This drives a set of coupled differential equations:

$$i\frac{da_{L\Lambda}(t)}{dt} = \sum_{K\Lambda} a_{K\Lambda}(t) \left(\langle \psi_{L\Lambda} | H^{el} | \psi_{K\Lambda} \rangle - i\frac{vZ}{R} \left\langle \psi_{L\Lambda} \middle| \frac{\partial}{\partial R} \middle| \psi_{K\Lambda} \right\rangle - i\frac{vb}{R^2} \langle \psi_{L\Lambda} | iLy | \psi_{K\Lambda} \rangle \right) \exp\left(-i \int_0^t (\varepsilon_{K\Lambda} - \varepsilon_{L\Lambda}) dt'\right) \quad (2\text{-}3)$$

including the radial NACME $\langle \psi_{K\Lambda} | \partial/\partial R | \psi_{L\Lambda} \rangle$ between molecular states of the same symmetry, and the rotational couplings $\langle \psi_{K\Lambda} | iLy | \psi_{L\Lambda} \rangle$ between states of different space symmetry. The present molecular calculation being performed in the C1 symmetry group, only radial NACME $\langle \psi_K | \partial/\partial R | \psi_L \rangle$ has to be taken into account. In the adiabatic representation, the first term equals zero.

The probability amplitudes a_K are deduced by integration of eq 2-3. The probabilities $P(b,v) = \Sigma_K |a_K(b,v,\infty)|^2$ are determined by summation over all charge transfer channels and cross sections are given by integration over the impact parameter.

The collision treatment was performed from ∼6 eV to ∼12 keV impact energies by means of the EIKONXS program.[50] The coupled equations have been solved assuming a 10^{-4} accuracy for the symmetry of the S matrix. All radial coupling transitions have been considered in the calculation. The anisotropy of the process has been taken into account by calculating the charge transfer cross sections for a proton approach along the three xyz axes. This may exhibit the behavior of the collision system in both perpendicular and in-the-plane orientations.

3. RESULTS AND DISCUSSION

The process may be analyzed looking first at the interactions between the molecular states involved. The potential energies in the collision of protons with 2-aminooxazole in the perpendicular direction along z are presented in Figure 2. A significant avoided crossing is exhibited between the entry channel and the highly excited charge transfer level of $\{(\pi_z^{NC})^2$

DOI: 10.1021/jp511658n
J. Phys. Chem. A XXXX, XXX, XXX−XXX

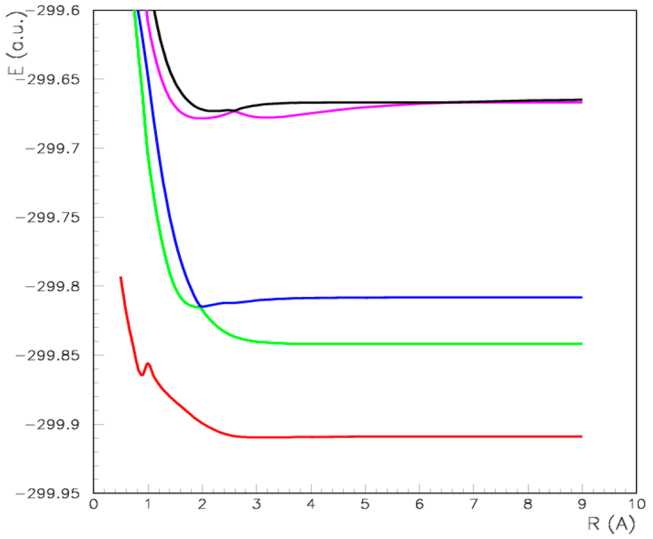

Figure 2. Adiabatic potential energy curves of the ^{1}A states in the collision of protons with 2-aminooxazoleymine in the perpendicular geometry: "red", $\{(\pi_z^{NC})^2\ (2p_{xy}^{N})^2\ \pi_{C1C2}\ 1s^H\}$; "green", $\{(\pi_z^{NC})^2\ 2p_{xy}^{N}\ (\pi_{C1C2})^2\ 1s^H\}$; "blue",$\{\pi_z^{NC}\ (2p_{xy}^{N})^2\ (\pi_{C1C2})^2\ 1s^H\}$; "magenta" $\{(\pi_z^{NC})^2\ 2p_{xy}^{N}\ \pi_{C1C2}\ p_z^{C}\ 1s^H\}$; "black", $\{(\pi_z^{NC})^2\ (2p_{xy}^{N})^2\ (\pi_{C1C2})^2\}$ configuration, entrance channel H^+ + 2-aminooxazole.

$2p_{xy}^{N}\ \pi_{C1C2}\ p_z^{C}\ 1s^H\}$ configuration, but the most important interaction appears around R = 2 au between the $\{\pi_z^{NC}\ (2p_{xy}^{N})^2\ (\pi_{C1C2})^2\ 1s^H\}$ and $\{(\pi_z^{NC})^2\ 2p_{xy}^{N}\ (\pi_{C1C2})^2\ 1s^H\}$ charge transfer states. The most important molecular orbitals involved in the process are indeed displayed in Figure 3. As already observed

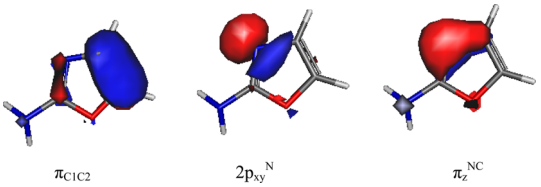

Figure 3. Main molecular orbitals involved in the charge transfer process.

for uracil and thymine targets,[24,27] the π orbital delocalized on the C1−C2 double bond clearly has to be pointed out, but an important role is devoted to the so-called π_z^{NC} orbital, which is widely delocalized on the C3−N1 and N1−C2 bonds, as shown in Figure 3, and is involved in the most important charge transfer level. The potential energy curves for the in-the-plane collision process are displayed in Figure 4. A quite different behavior may be pointed out with regard to the perpendicular approach. First of all, the $\{(\pi_z^{NC})^2\ 2p_{xy}^{N}\ \pi_{C1C2}\ p_z^{C}\ 1s^H\}$ charge transfer level is higher in energy, and no direct interaction with the entry channel may be exhibited. However, the three charge transfer levels involved in the process present quite strong avoided crossings, which could drive efficient electron exchange. They appear a bit shifted to longer R distances in the in-the-plane collision, and important avoided crossings corresponding to successive single excitations may be pointed out between the entrance channel and charge transfer ones.

The collision treatment has been performed for an approach of the proton along the three *xyz* axes in order to consider the orientation dependence of the process. The corresponding partial cross sections are presented in Figure 5 and Table 2. The charge transfer process seems to be more efficient when

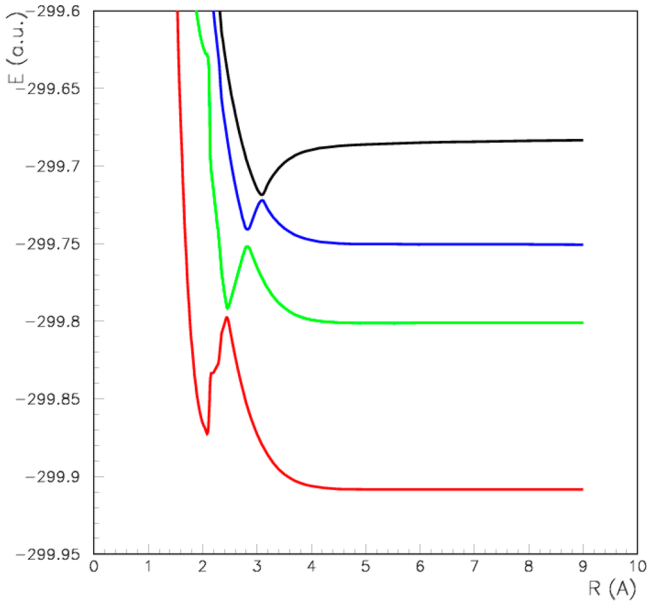

Figure 4. Adiabatic potential energy curves of the ^{1}A states in the collision of protons with 2-aminooxazoleymine in the ring plane along the *y* axis: "red", $\{(\pi_z^{NC})^2\ (2p_{xy}^{N})^2\ \pi_{C1C2}\ 1s^H\}$; "green", $\{(\pi_z^{NC})^2\ 2p_{xy}^{N}\ (\pi_{C1C2})^2\ 1s^H\}$; "blue",$\{\pi_z^{NC}\ (2p_{xy}^{N})^2\ (\pi_{C1C2})^2\ 1s^H\}$; "black", $\{(\pi_z^{NC})^2\ (2p_{xy}^{N})^2\ (\pi_{C1C2})^2\}$ configuration, entrance channel H^+ + 2-aminooxazole.

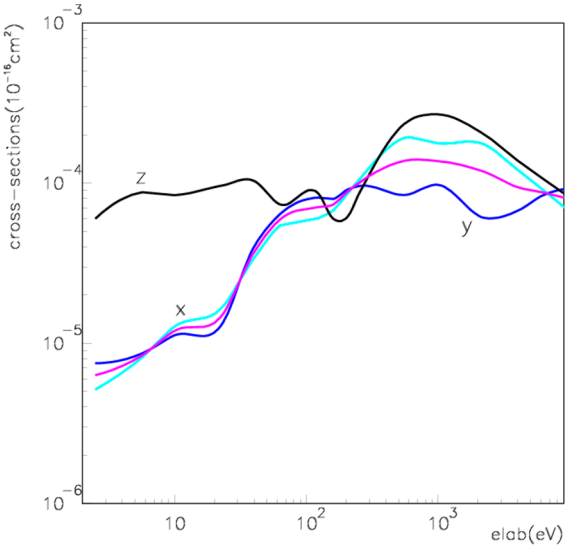

Figure 5. Charge transfer cross sections in the collision of protons with 2-aminooxazole along the *xyz* axes: "black", *z* axis (perpendicular orientation); "light blue", *x* axis; "blue", *y* axis; "magenta", mean in-the-plane value.

the proton is colliding with the 2-aminooxazole target in the perpendicular orientation. This is particularly effective at very low eV impact energies, where the charge transfer cross sections are higher by about an order of magnitude in the perpendicular geometry than in planar collisions along *x* and *y*. However, for collisions energies higher than 60−100 eV, the in-the-plane charge transfer process shows an increasing efficiency and reaches the same order of magnitude observed for the perpendicular orientation, on the order of $10^{-4} \times 10^{-16}$ cm^2 with a maximum at $2.7 \times 10^{-4} \times 10^{-16}$ cm^2 along *z*. The process, however, remains less favored for in-the-plane

DOI: 10.1021/jp511658n
J. Phys. Chem. A XXXX, XXX, XXX−XXX

Table 2. Charge Transfer Cross Sections for the Collision of 2-Aminooxazole with Protons on the *x*, *y*, *z* axes (in 10^{-16}cm^2)

velocity (a.u.)	E_{lab} (eV)	along *x*	along *y*	along *z*
0.015	5.7	8.22×10^{-6}	8.67×10^{-6}	8.78×10^{-5}
0.02	10.0	1.27×10^{-5}	1.12×10^{-5}	8.43×10^{-5}
0.03	22.6	1.66×10^{-5}	1.30×10^{-5}	9.63×10^{-5}
0.04	40.0	3.40×10^{-5}	3.99×10^{-5}	1.03×10^{-4}
0.05	63.0	5.45×10^{-5}	6.40×10^{-5}	7.37×10^{-5}
0.07	123.4	6.05×10^{-5}	8.13×10^{-5}	8.60×10^{-5}
0.08	161.1	6.81×10^{-5}	7.96×10^{-5}	5.98×10^{-5}
0.09	203.9	8.54×10^{-5}	9.10×10^{-5}	6.13×10^{-5}
0.1	251.8	1.06×10^{-4}	9.60×10^{-5}	8.65×10^{-5}
0.15	566.5	1.92×10^{-4}	8.45×10^{-5}	2.38×10^{-4}
0.2	1.0×10^3	1.77×10^{-4}	9.76×10^{-5}	2.69×10^{-4}
0.3	2.3×10^3	1.74×10^{-4}	6.06×10^{-5}	2.00×10^{-4}
0.4	4.0×10^3	1.22×10^{-4}	6.71×10^{-5}	1.39×10^{-4}
0.5	6.3×10^3	9.04×10^{-5}	8.42×10^{-5}	1.06×10^{-4}
0.6	9.1×10^3	7.08×10^{-5}	9.18×10^{-5}	8.60×10^{-5}
0.7	12.3×10^3	5.71×10^{-5}	9.33×10^{-5}	7.14×10^{-5}

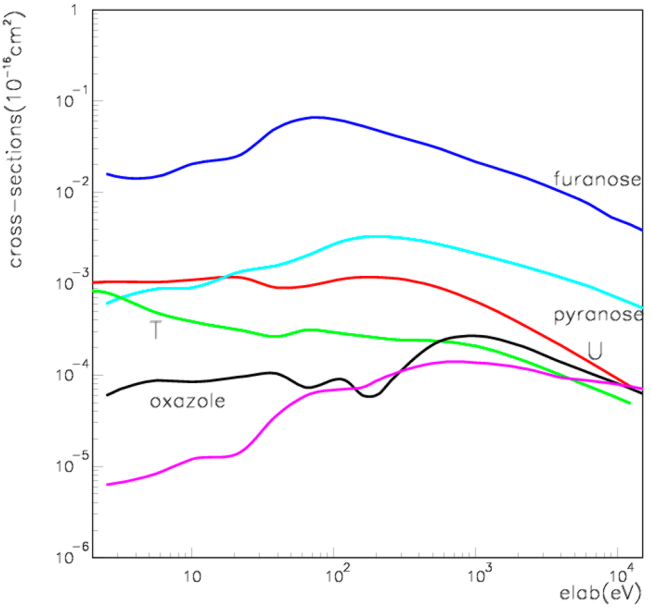

Figure 6. Charge transfer cross sections for collisions of protons with biomolecular targets: "green", thymine; "red", uracil; "blue", 2-deoxy-D-ribose-furanose form; "light blue", 2-deoxy-D-ribose-pyranose form; "black", 2-aminooxazole, perpendicular approach; "magenta", 2-aminooxazole, planar approach.

approaches, as shown in the main values. Such evidence has already been pointed out for the DNA and RNA building blocks pyrimidine nucleobases[25−27] and 2-deoxy-D-ribose[29] and appears to be a general feature in those charge transfer processes, in a wide collision energy range.[28,37]

These results may be compared to the collisions of protons with DNA and RNA building blocks. Effectively, a previous study on collisions of protons on uracil, thymine, and 2-deoxy-D-ribose has shown lower charge transfer cross sections for the pyrimidine nucleobases.[31] Furthermore, calculations for furanose (five-membered ring) and pyranose (six-membered ring) conformations of the 2-deoxy-D-ribose have pointed out a significant dependence on the conformation of the biomolecular target.[31,32] The comparison of this series of biomolecular targets could thus drive some general trends with regard to the behavior of the 2-aminooxazole prebiotic species, in particular in their resistance in proton-rich environments. The charge transfer cross sections for the different biological targets are displayed in Figure 6. Clearly, the electron capture in proton collisions appears to be even less efficient for 2-aminooxazole targets than for pyrimidine nucleobases, in particular at lower collision energies. It appears to be of the same order of magnitude in the keV collision range. This may indeed drive significant implication on the resistance of this hypothetical prebiotic compound to spatial radiation and consequently its survival in space. Effectively, if one considers the different processes induced by the impact of a projectile ion on a target, the relative fragmentation yield of the ionized species and the corresponding charge transfer cross sections have been shown to have opposite variations,[21] as widely pointed out previously.[26,31,37] So a lower electron exchange cross sections could thus suggest that 2-aminooxazole would be more sensitive in proton collisions than pyrimidine DNA and RNA nucleobases, and *a fortiori* than the sugar moiety, whatever its conformation. 2-Aminooxazole would thus be more easily disintegrated in proton collisions. Such analysis is of course quite qualitative, but an enhanced fragmentation might question the resistance of such a prebiotic intermediate, more specifically in proton-rich regions like H II, and thus its key role in the reaction sequence at the origin of life. This discussion concerns yet gas phase processes, with regard to the theoretical treatment of course, but also with regard to measurements that come from gas phase experiments.[19−21] Important interest may also be devoted to reactions involving water, as processes occurring at the surface of icy grains or even processes occurring in bulk aqueous early earth environments. Solvation effects might be determinant to drive conclusions on given species at the origin of life. Investigation of the photochemistry of 2-aminooxazole has indeed suggested an enhanced photostability in water solvent.[13] A treatment taking into account solute−solvent interactions with a controlled analysis of water clusters toward the first hydration shell would be of fundamental interest and is a future step.

4. CONCLUDING REMARKS

The charge transfer process in collisions of protons with 2-aminooxazole has been studied by means of ab initio quantum chemical calculations followed by a semiclassical treatment in the eV to keV collision energy range. A compared analysis with different targets, pyrimidine nucleobases and 2-deoxy-D-ribose in furanose and pyranose forms, which could be possible building blocks at early stages of life, has been performed, and some qualitative trends could be exhibited. In the gas phase, the 2-aminooxazole exhibits a clear sensitivity in proton collisions, which could drive a significant weakness under spatial radiations. Such features would not be favorable for the survival of this compound in space, especially in proton-rich regions. Further investigations have to be developed with regard to early earth environments with, in particular, consideration of water solvation.

■ ASSOCIATED CONTENT

Supporting Information

The optimized geometries of 2-aminooxazole and its cation are available free of charge via the Internet at http://pubs.acs.org.

DOI: 10.1021/jp511658n
J. Phys. Chem. A XXXX, XXX, XXX−XXX

AUTHOR INFORMATION

Corresponding Author

*E-mail: bacchus@univ-lyon1.fr; tel: +33472431083.

Notes

The authors declare no competing financial interest.

ACKNOWLEDGMENTS

We acknowledge support from the HPC resources of CCRT/CINES/IDRIS under the allocation 2014-[i2014081566] made by GENCI [Grand Equipement National de Calcul Intensif] and from the COST actions TD1308 Life-ORIGINS, CM1204 XLIC, and MP1002 Nano-IBCT.

REFERENCES

(1) Miller, S. L. Production of Some Organic Compounds under Possible Primitive Earth Conditions. *J. Am. Chem. Soc.* **1953**, *77*, 2351−2361.

(2) Miller, S. L.; Hurey, H. C. Organic Compound Synthesis on the Primitive Earth. *Science* **1959**, *130*, 245−251.

(3) De Marcellus, P.; Bertrand, M.; Nuevo, M.; Westall, F.; d'Hendecourt, L. L. Prebiotic Significance of Extraterrestrial Ice Photochemistry: Detection of Hydantoin in Organic Residues. *Astrobiology* **2011**, *11*, 847−854.

(4) Huber, C.; Eisenreich, W.; Hecht, S.; Wächtershäuser, G. A Possible Primordial Peptide Cycle. *Science* **2003**, *301*, 938−940.

(5) Crick, F. H. C. The Origin of the Genetic Code. *J. Mol. Biol.* **1968**, *38*, 367−379.

(6) Orgel, L. E. Evolution of the Genetic Apparatus. *J. Mol. Biol.* **1968**, *38*, 381−393.

(7) Joyce, G. F. The Antiquity of RNA-Based Evolution. *Nature* **2002**, *418*, 214−221.

(8) Powner, M. W.; Gerland, B.; Sutherland, J. D. Synthesis of Activated Pyrimidine Ribonucleotides in Prebiotically Plausible Conditions. *Nature* **2009**, *459*, 239−242.

(9) Powner, M. W.; Sutherland, J. D. Prebiotic Chemistry: A New Modus Operandi. *Philos. Trans. R. Soc. B* **2011**, *366*, 2870−2877.

(10) Islam, S.; Aguilar, J. A.; Powner, M. W.; Nilsson, M.; Morris, G. A.; Sutherland, J. D. Detection of Potential TNA and RNA Nucleoside Precursors in a Prebiotic Mixture by Pure Shift Diffusion-Ordered NMR Spectroscopy. *Chem.—Eur. J.* **2013**, *19*, 4586−4595.

(11) Møllendal, H.; Konovalov, A. Microwave Spectrum of 2-Aminooxazole, a Compound of Potential Prebiotic and Astrochemical Interest. *J. Phys. Chem. A* **2010**, *114*, 2151−2156.

(12) Szabla, R.; Šponer, J. E.; Šponer, J.; Góra, R. W. Theoretical Studies of the Mechanism of 2-Aminooxazole Formation under Prebiotically Plausible Conditions. *Phys. Chem. Chem. Phys.* **2013**, *15*, 7812−7818.

(13) Szabla, R.; Tuna, D.; Góra, R. W.; Šponer, J.; Sobolewski, A. L.; Domke, W. Photochemistry of 2-Aminooxazole, a Hypothetical Prebiotic Precursor of RNA Nucleotides. *J. Phys. Chem. Lett.* **2013**, *4*, 2785−2788.

(14) Cooper, G. W.; Onwo, W. M.; Cronin, J. R. Alkyl Phosphoric Acids and Sulfonic Acids in the Murchison Meteorite. *Geochim. Cosmochim. Acta* **1992**, *56*, 4109−4115.

(15) Ehrenfreund, P.; Bernstein, M.; Dworkin, J.; Sandford, S. A.; Allamandola, L. J. The Photostability of Amino Acids in Space. *Astrophys. J.* **2001**, *550*, L95−L99.

(16) Ehrenfreund, P.; Irvine, W.; Becker, L.; Blank, J.; Brucato, R.; Colangeli, L.; Derenne, S.; Despois, D.; Dutrey, A.; Fraaije, H.; Lazcano, A.; Owen, T.; Robert, F. Astrophysical and Astrochemical Insights into the Origin of Life. *Rep. Prog. Phys.* **2002**, *65*, 1427−1488.

(17) von Sonntag, C. *The Chemical Basis for Radiation Biology*; Taylor and Francis: London, 1987.

(18) Michael, B. D.; O'Neill, P. D. A Sting in the Tail of Electron Tracks. *Science* **2000**, *287*, 1603−1604.

(19) Coupier, B.; Farizon, B.; Farizon, M.; Gaillard, M. J.; Gobet, F.; de Castro Faria, N. V.; Jalbert, G.; Ouaskit, S.; Carré, M.; Gstir, B.; et al. Inelastic Interactions of Protons and Electrons with Biologically Relevant Molecules. *Eur. Phys. J. D* **2002**, *20*, 459−468.

(20) de Vries, J.; Hoekstra, R.; Morgenstern, R.; Schlathölter, T. Multiple Ionization and Fragmentation of the DNA Base Thymine by Interaction with C^{q+} Ions. *Eur. Phys. J. D* **2003**, *24*, 161−164.

(21) Alvarado, F.; Bari, S.; Hoekstra, R.; Schlathölter, T. Quantification of Ion-Induced Molecular Fragmentation of Isolated 2-Deoxy-D-ribose Molecules. *Phys. Chem. Chem. Phys.* **2006**, *8*, 1922−1928.

(22) Deng, Z.; Imhoff, M.; Huels, M. A. Fragmentation Dynamics of Condensed Phase Thymine by Low-Energy (10−200 eV) Heavy-Ion Impact. *J. Chem. Phys.* **2005**, *123*, 144509.

(23) Deng, Z.; Bald, I.; Illenberger, E.; Huels, M. A. Beyond the Bragg Peak: Hyperthermal Heavy Ion Damage to DNA Components. *Phys. Rev. Lett.* **2005**, *95*, 153201.

(24) Bacchus-Montabonel, M. C.; Łabuda, M.; Tergiman, Y. S.; Sienkiewicz, J. E. Theoretical Treatment of Charge-Transfer Processes Induced by Collision of C^{q+} Ions with Uracil. *Phys. Rev. A* **2005**, *72*, 052706.

(25) Bacchus-Montabonel, M. C.; Tergiman, Y. S. Anisotropic Effect in the Charge Transfer of C^{q+} Ions with Uracil. *Phys. Rev. A* **2006**, *74*, 054702.

(26) Bacchus-Montabonel, M. C.; Tergiman, Y. S.; Talbi, D. An-Initio Molecular Treatment of Charge-Transfer Processes Induced by Collision of Carbon Ions with 5-Halouracil Molecules. *Phys. Rev. A* **2009**, *79*, 012710.

(27) Bacchus-Montabonel, M. C.; Tergiman, Y. S. An Ab-Initio Study of Ion Induced Charge Transfer Dynamics in Collision of Carbon Ions with Thymine. *Phys. Chem. Chem. Phys.* **2011**, *13*, 9761−9767.

(28) Bacchus-Montabonel, M. C.; Tergiman, Y. S. Charge Transfer Dynamics of Carbon Ions with Uracil and Halouracil Targets at Low Collision Energies. *Chem. Phys. Lett.* **2011**, *503*, 45−48.

(29) Bacchus-Montabonel, M. C. Ab-Initio Treatment of Ion-Induced Charge Transfer Dynamics of Isolated 2-Deoxy-D-ribose. *J. Phys. Chem. A* **2014**, *118*, 6326−6332.

(30) Bacchus-Montabonel, M. C. Radiative and Collisional Processes in Space Chemistry. *Rend. Fis. Accad. Lincei* **2011**, *22*, 95−103.

(31) Bacchus-Montabonel, M. C. Looking at Radiation Damage on Prebiotic Building Blocks. *J. Phys. Chem. A* **2013**, *117*, 14169−14175.

(32) Hervé du Penhoat, M. A.; Lopez-Tarifa, P.; Ghose, K. K.; Jeanvoine, Y.; Gaigeot, M. P.; Vuilleumier, R.; Politis, M. F.; Bacchus-Montabonel, M. C. Modeling Proton-Induced Damage on 2-Deoxy-D-ribose. Conformational Analysis. *J. Mol. Model.* **2014**, *20*, 2221.

(33) López-Tarifa, P.; Hervé du Penhoat, M. A.; Vuilleumier, R.; Gaigeot, M. P.; Tavernelli, I.; Le Padellec, A.; Champeaux, J. P.; Alcamí, M.; Moretto-Capelle, P.; Martín, F.; Politis, M. F. Ultrafast Nonadiabatic Fragmentation Dynamics of Doubly Charged Uracil in a Gas Phase. *Phys. Rev. Lett.* **2011**, *107*, 023202.

(34) López-Tarifa, P.; Gaigeot, M. P.; Vuilleumier, R.; Tavernelli, I.; Alcamí, M.; Martín, F.; Hervé du Penhoat, M. A.; Politis, M. F. Ultrafast Damage Following Radiation-Induced Oxidation of Uracil in Aqueous Solution. *Angew. Chem.* **2013**, *125*, 3242−3245; *Angw. Chem. Int. Ed.* **2013**, *52*, 3160−3163.

(35) Bacchus-Montabonel, M. C.; Tergiman, Y. S. Charge Transfer Rate Coefficients in Collision of C^{2+} Ions with CO and N_2 Molecular Targets. *Chem. Phys. Lett.* **2010**, *497*, 18−21.

(36) Bacchus-Montabonel, M. C. Theoretical Study of Charge Transfer Dynamics in Collisions of C^{6+} Carbon Ions with Pyrimidine Nucleobases. *Eur. Phys. J. D* **2012**, *66*, 175.

(37) Bacchus-Montabonel, M. C.; Tergiman, Y. S. Radiation Damage on Biomolecular Systems: Dynamics of Ion Induced Collision Processes. *Comput. Theor. Chem.* **2012**, *990*, 177−184.

(38) Salem, L. *Electrons in Chemical Reactions: First Principles*; Wiley Interscience: New York, 1982.

(39) Bacchus-Montabonel, M. C.; Talbi, D.; Persico, M. Quantum Chemical Determination of the Rate Coefficients for Radiative Association of CH_3^+ and H_2. *J. Phys. B* **2000**, *33*, 955−959.

DOI: 10.1021/jp511658n
J. Phys. Chem. A XXXX, XXX, XXX−XXX

513 (40) Bene, E.; Martinez, P.; Halász, G. J.; Vibók, Á; Bacchus-
514 Montabonel, M. C. Charge Transfer in Collisions of C^{2+} carbon Ions
515 with CO and OH Targets. *Phys. Rev. A* **2009**, *80*, 012711.
516 (41) Werner, H. J.; Knowles, P. J. MOLPRO Package of Ab Initio
517 Programs (version 2012.1).
518 (42) Wetmore, S. D.; Boyd, R. J.; Eriksson, L. A. A Theoretical Study
519 of 5-Halouracils: Electron Affinities, Ionization Potentials and
520 Dissociation of the Related Anions. *Chem. Phys. Lett.* **2001**, *343*,
521 151−158.
522 (43) Bacchus-Montabonel, M. C.; Wiesenfeld, L. Analysis of the
523 Formation of CH^+ in Collision of C^{2+} Ions with Molecular Hydrogen.
524 *Chem. Phys. Lett.* **2013**, *583*, 23−27.
525 (44) Honvault, P.; Gargaud, M.; Bacchus-Montabonel, M. C.;
526 McCarroll, R. Recombination of O^{2+} Ions by Electron Capture from
527 Atomic Hydrogen in Photoionized Nebulae. *Astron. Astrophys.* **1995**,
528 *302*, 931−934.
529 (45) Bacchus-Montabonel, M. C. Ab Initio Potential-Energy Curves
530 and Radial and Rotational Couplings for the Process $N^{5+} + He \rightarrow N^{4+}$
531 $+ He^+$. *Phys. Rev. A* **1987**, *36*, 1994−2001.
532 (46) Stancil, P. C.; Zygelman, B.; Kirby, K. *Photonic, Electronic, and*
533 *Atomic Collisions*; Aumayr, F., Winter, H.P., Eds.; World Scientific:
534 Singapore, 1998; p 537.
535 (47) Sidis, V. Vibronic Phenomena in Collisions of Atomic and
536 Molecular Species. *Adv. At. Mol. Opt. Phys.* **1990**, *26*, 161−208.
537 (48) Chenel, A.; Mangaud, E.; Justum, Y.; Talbi, D.; Bacchus-
538 Montabonel, M. C.; Desouter-Lecomte, M. Quantum Dynamics of the
539 Charge Transfer in $C^+ + S$ at Low Collision Energies. *J. Phys. B* **2010**,
540 *43*, 245701.
541 (49) Linguerri, R.; Hochlaf, M.; Bacchus-Montabonel, M. C.;
542 Desouter-Lecomte, M. Characterization of the MgO^{2+} Dication in
543 the Gas Phase: Electronic States, Spectroscopy and Atmospheric
544 Implications. *Phys. Chem. Chem. Phys.* **2013**, *15*, 824−831.
545 (50) Allan, R. J.; Courbin, C.; Salas, P.; Wahnon, P. State-Selective
546 Effects in the Differential Cross section for Electron Capture from
547 Laser-Excited Sodium Atoms by Protons. *J. Phys. B* **1990**, *23*, L461−
548 L466 http://www.ccp6.ac.uk/downloads/eikonxs.htm.

DOI: 10.1021/jp511658n
J. Phys. Chem. A XXXX, XXX, XXX−XXX